Improved Retinal Function in a Mouse Model of Dominant Retinitis Pigmentosa Following AAV-delivered Gene Therapy

Naomi Chadderton[1], Sophia Millington-Ward[1], Arpad Palfi[1], Mary O'Reilly[1], Gearóid Tuohy[1], Marian M Humphries[1], Tiansen Li[2], Peter Humphries[1], Paul F Kenna[1,3] and G Jane Farrar[1]

[1]Department of Genetics, Smurfit Institute of Genetics, Trinity College Dublin, Dublin 2, Ireland; [2]Department of Ophthalmology, Harvard Medical School, Massachusetts Eye and Ear Infirmary, Boston, Massachusetts, USA; [3]Research Foundation, Eye and Ear Hospital, Dublin, Ireland

Mutational heterogeneity represents one of the greatest barriers impeding the progress toward the clinic of gene therapies for many dominantly inherited disorders. A general strategy of gene suppression in conjunction with replacement has been proposed to overcome this mutational heterogeneity. In the current study, various aspects of this strategy are explored for a dominant form of the retinal degeneration, retinitis pigmentosa (RP), caused by mutations in the rhodopsin gene (*RHO-adRP*). While >200 mutations have been identified in rhodopsin (RHO), in principle, suppression and replacement may be employed to provide a single mutation-independent therapeutic for this form of the disorder. In the study we demonstrate in a transgenic mouse simulating human *RHO*-adRP that RNA interference–based suppression, together with gene replacement utilizing the endogenous mouse gene as the replacement, provides significant benefit as evaluated by electroretinography (ERG). Moreover, this is mirrored histologically by preservation of photoreceptors. AAV-based vectors were utilized for *in vivo* delivery of the therapy to the target cell type, the photoreceptors. The results demonstrate that RNAi-based mutation-independent suppression and replacement can provide benefit for *RHO*-adRP and promote the therapeutic approach as potentially beneficial for other autosomal dominantly inherited disorders.

Received 12 November 2008; accepted 17 December 2008; published online 27 January 2009. doi:10.1038/mt.2008.301

INTRODUCTION

During 2007, three phase I human clinical trials commenced for a debilitating recessive retinal disorder, Leber's congenital amaurosis. These initial findings[1–3] have been fundamental in establishing the safety of subretinal AAV delivery to humans, representing a milestone in ocular gene therapy.

By contrast, therapeutic developments for autosomal dominant retinal disorders have not proceeded at the same pace, largely due to their inherent complexity. Therapeutic approaches under consideration include strategies to modulate secondary effects associated with disease such as factors influencing cell longevity or function.[4–8] However, many dominantly inherited disorders may require correction of the underlying genetic defect. Furthermore, these dominant disorders typically demonstrate significant mutational heterogeneity rendering the development of most mutation-specific gene therapies neither economically nor technically feasible. Therefore, the methodologies that circumvent mutational heterogeneity, while still correcting the primary genetic defect, would be extremely valuable. A strategy of gene suppression in conjunction with gene replacement, in essence a two-component therapy that is mutation independent, has been proposed.[9–13] The strategy involves suppression of both mutant and wild-type alleles of a target gene and simultaneous provision of a replacement gene that encodes wild-type protein but is refractory to suppression, due to sequence changes at degenerate sites.[13,14]

Retinitis pigmentosa [RP (MIM 180380)], a retinopathy affecting 1 in 3,000 people, involves rod photoreceptor cell death causing loss of night and peripheral vision. Subsequently, cones degenerate, giving rise to loss of central vision.[15] Rhodopsin (RHO)-based autosomal domiant RP [*RHO*-adRP (GenBank accession no. NM_000539.2)], a common form of RP, has been the focus of much attention since the initial identification of the disease-causing gene almost two decades ago.[16–18] *RHO*-adRP is mutationally heterogeneous (Retinal Information Network database), a situation mirrored in many dominantly inherited conditions (OMIM database) such as collagen-linked Osteogenesis Imperfecta (MIM 166210) and Epidermolysis Bullosa (MIM 131750). Because many RHO mutations have been shown to be dominant negative[19] and studies with transgenic mice have demonstrated that lower levels of mutant RHO is associated with less severe disease,[20] *RHO*-adRP represents a model disorder for suppression and replacement gene therapy.

Previous studies for *RHO*-adRP have been focused on mutation-specific[21–23] or mutation-independent suppression of RHO using ribozymes[24,25] or RNAi.[12,26] In addition, aspects of RNAi-mediated suppression in conjunction with codon-modified gene replacement therapy have been explored.[13,27] However, while histological benefit was observed, due in part to the rapid nature of

The first two authors contributed equally to this work.

Correspondence: *Naomi Chadderton, Smurfit Institute of Genetics, Trinity College Dublin, Dublin 2, Ireland. E-mail: chaddern@tcd.ie*

the retinopathy in the mouse model used,[20] no functional benefit was demonstrated by electroretinography (ERG).

In the current study, we set out to determine what effects suppression and replacement would have on retinal function, as assessed by ERG. Recombinant AAV2/5 viruses (AAV) with RNAi-based suppressors have been generated, the choice of AAV serotype being determined by the predeliction of the virus for photoreceptors.[28–30] Following subretinal administration of AAV vectors, potent suppression of RHO was achieved in a transgenic mouse carrying a wild-type human *RHO* transgene (the NHR mouse[20]), resulting in compromised histology and ERG. In addition, suppression and replacement was addressed in a transgenic mouse simulating human *RHO*-adRP, the Pro347Ser mouse.[31] Critically AAV-delivered RNAi-based suppression in the presence of expression of an endogenous mouse RHO gene (*Rho*) refractory to suppression (due to sequence divergence between mouse and human) improves retinal histology and function in Pro347Ser mice, the latter being evaluated by ERG. The current study provides a clear demonstration that RNAi-based suppression in conjunction with codon-modified gene replacement can provide ERG benefit in an animal model of a dominant retinal disease and further validates this strategy as a means to overcome the significant mutational hetergeneity present in many dominantly inherited conditions.

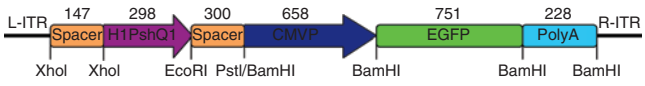

Figure 1 Schematic representation of the AAVshQ1 suppression construct. shQ1 RNA was expressed from the H1 promoter (H1shQ1). The H1shQ1 cassette was flanked up- and down-stream by spacer DNA fragments. EGFP was coexpressed from the CMV immediate-early promoter (CMVP). The SV40 polyadenylation signal (PolyA) was located at the 3′ end of the *EGFP* gene. Restriction enzyme sites used for cloning are given. Numbers indicate molecular sizes in base pairs, and arrows indicate the direction of transcription. L-ITR and R-ITR: left and right inverted repeats of AAV.

RESULTS

Evaluation of RNAi-mediated suppression of RHO has previously been undertaken in cell culture, thereby resulting in the characterization of efficient suppression molecules.[13,27] A potent RNAi suppressor termed Q1, shown to suppress RHO in HeLa cells and retinal explants by >80%, has been generated as a short hairpin RNA (shQ1) in an AAV vector (AAVshQ1; **Figure 1**). In addition, a control AAV vector with a nontargeting RNAi molecule was produced (AAVshNT). Both AAV viruses also incorporate an EGFP reporter gene as a marker for AAV transduction and to enable isolation of transduced cell populations by fluorescent-activated cell sorting (FACS). AAVshQ1 was subretinally injected into adult wild-type mice and retinal RNA extracted after 10 days. RNase protection assays demonstrated expression of the 21-nucleotide shQ1 *in vivo* (**Figure 2a**).

To establish whether AAVshQ1 suppresses human RHO *in vivo*, the NHR mouse expressing a normal RHO transgene on a mouse Rho knockout background was used ($RHO^{+/-}Rho^{-/-}$; refs 20,32). These NHR mice have retinal histology and ERG akin to wild-type mice.[27] AAVshQ1 and AAVshNT were subretinally injected into fellow eyes of adult NHR mice ($n = 4$). Four weeks after administration of virus, retinal cells were dissociated and EGFP-expressing cells were sorted by FACS to isolate AAV-transduced cells (**Figure 2b**), RNA were extracted, and RHO mRNA expression levels were determined by quantitative real-time reverse

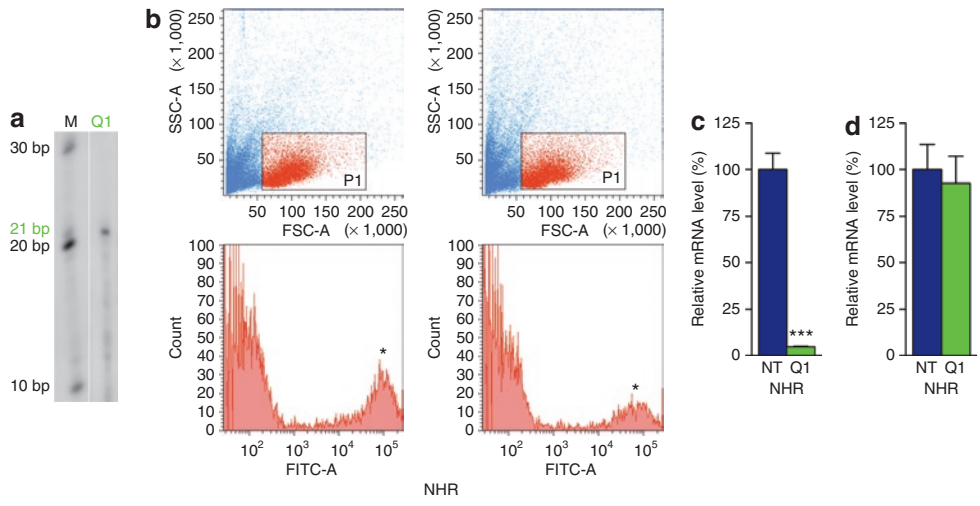

Figure 2 Suppression of human and mouse rhodopsin *in vivo*. Fellow eyes of NHR ($RHO^{+/-}Rho^{-/-}$) and wild-type ($Rho^{+/+}$) mice were subretinally injected with 2 µl of 2×10^{12} vp/ml AAVshQ1, which enables coexpression of shQ1 and EGFP in transduced retinal cells. (**a**) Expression of the 21-nucleotide (nt) shQ1 was confirmed by RNase protection assay in adult mice 10 days postinjection ($n = 2$). Protected RNA was separated on 15% denaturing polyacrylamide gels and detected using an shQ1 RNA probe, labeled with P^{32}-γATP (lane Q1). In lane M, size markers indicate 10, 20, and 30 nt. Four weeks after AAVshNT (NT) and AAVshQ1 (Q1) administration at postnatal day 10, retinas were dissociated with trypsin and retinal cells sorted and analyzed by FACS ($n = 4$). (**b**) Representative plots of forward versus side scatter and histograms of EGFP fluorescence of the gated population (red dots on scatter plots) of NHR retinas are given for both AAVshNT (NT) and AAVshQ1 (Q1). (**c**) The bar chart indicates RHO mRNA expression from NHR mice in AAV-transduced (EGFP-positive) cells expressing shNT (NT) and shQ1 (Q1), isolated by FACS and quantified by qRT-PCR. (**d**) The bar chart indicates Rho mRNA expression from $Rho^{+/+}$ mice in AAV-transduced (EGFP-positive) cells expressing shNT (NT) and shQ1 (Q1), isolated by FACS and quantified by qRT-PCR. Error bars represent SD values. *EGFP-positive fraction of cells; ***$P < 0.001$.

transcription PCR (qRT-PCR). Notably, RHO mRNA levels in the transduced populations were suppressed *in vivo* by 95% (expression level of 4.7 ± 0.3%, $P < 0.001$, **Figure 2c**). Human RHO expression in NHR mice revealed that RHO is expressed at ~70% the level of expression of the endogenous mouse *Rho* gene in wild-type mice.[13]

Whereas shQ1 targets the human RHO sequence, it contains four nucleotide mismatches to the mouse Rho sequence. To determine the specificity of shQ1 to human RHO versus mouse Rho, AAVshQ1 and AAVshNT were subretinally injected into fellow eyes of adult wild-type mice ($Rho^{+/+}$; $n = 4$). Ten days postinjection retinal cells were dissociated, EGFP-expressing cells were isolated by FACS, RNA were extracted, and Rho mRNA expression levels were determined by qRT-PCR. No significant suppression of mouse Rho was observed in wild-type mice ($Rho^{+/+}$) injected with shQ1 (**Figure 2d**). In contrast, as indicated above, shQ1 suppresses human RHO by 95% in NHR mice that express a human RHO transgene ($RHO^{+/-}Rho^{-/-}$; **Figure 2c**).

To further assess the *in vivo* effects of RNAi-mediated suppression of human RHO in NHR mice, eyes were subretinally injected with AAVshQ1 and AAVshNT at postnatal day 10 (P10) and analyzed 4 weeks later. A viral spread of 30–40% was observed after a single subretinal injection (data not shown). Histological analysis ($n = 3$) revealed a marked loss of photoreceptor cell segments and a substantial reduction of RHO immunolabeling in AAVshQ1-injected eyes (**Figure 3b,h**) compared to AAVshNT-injected (**Figure 3a,g**) and uninjected eyes (**Figure 3c,i**). Loss of photoreceptor cell segments in shQ1- versus shNT-expressing cells was also demonstrated by the EGFP expression pattern (**Figure 3d,g**, and **Figure 3e,h**). While EGFP-labeled photoreceptor segments were prevalent in AAVshNT-transduced retinas (**Figure 3d,g**), very few EGFP-positive photoreceptor segments were visible in AAVshQ1-transduced retinas (**Figure 3e,h**). Note that EGFP was not detected in uninjected retinas. To assess functional effects of RHO suppression, ERG was undertaken ($n = 6$). ERG of AAVshQ1- versus AAVshNT-injected eyes demonstrated that suppression of RHO resulted in significant reductions in rod-isolated (54.4 ± 27.3 and 100 ± 37.1%, respectively; $P < 0.05$), mixed rod and cone (52.7 ± 30.8 and 100 ± 42.1%, respectively; $P < 0.05$), and cone-isolated (48.9 ± 35.0 and 100 ± 44.8%, respectively; $P < 0.05$) responses (**Figure 3j**). This demonstrates clear functional effects of AAV-mediated RNAi-based suppression of RHO *in vivo*.

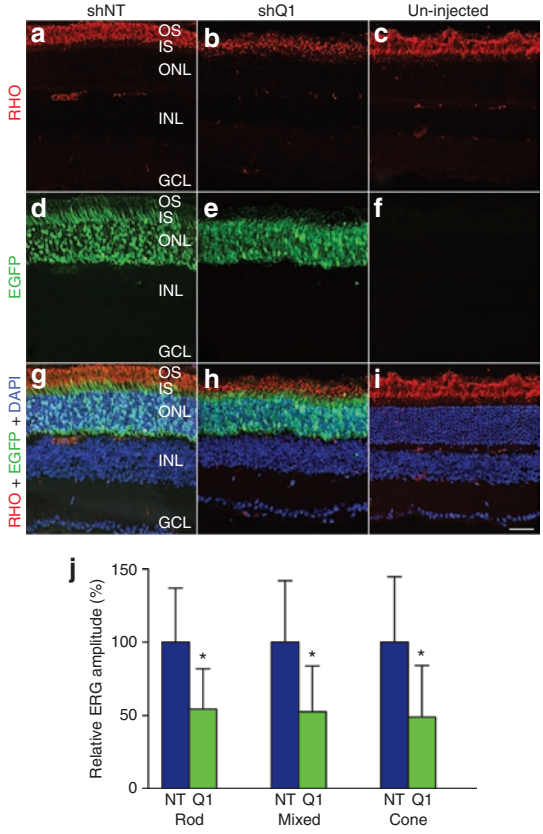

Figure 3 Retinal histology and ERG of NHR mice following suppression of RHO. Fellow eyes from NHR ($RHO^{+/-}Rho^{-/-}$) mice were injected with 2 µl 2 × 10^{12} of vp/ml AAVshQ1 and AAVshNT at postnatal day 10 and analyzed 4 weeks postinjection. For histology, eyes ($n = 3$) were fixed in 4% paraformaldehyde and cryosectioned (12 µm). Cy3 label RHO immunocytochemistry was carried out and nuclei counterstained with DAPI. Representative microscopic images are provided from eyes injected with AAVshNT (**a**, **d**, and **g**), AAVshQ1 (**b**, **e**, and **h**), and from uninjected eyes (**c**, **f**, and **i**). Red, green, and blue fluorescence corresponds to signals of RHO, EGFP, and cell nuclei, respectively. For ERG analysis ($n = 6$), mice were dark adapted over night and ERG responses recorded from both eyes. (**j**) Means of relative amplitudes of ERGs are given for rod-isolated (rod), mixed rod and cone (mixed), and cone-isolated (cone) responses corresponding to AAVshNT (NT) and AAVshQ1 (Q1) injections. OS, photoreceptor outer segments; IS, photoreceptor inner segments; ONL, outer nuclear layer; INL, inner nuclear layer; GCL, ganglion cell layer; Bar = 25 µm. Error bars correspond to SD values; *$P < 0.05$.

While functional effects of AAVshQ1 suppression were observed in NHR mice, it was a key objective of the study to explore whether suppression and replacement, the latter using the endogenous mouse gene resistant to suppression, translates to improved visual function in the context of an animal model that simulates the human condition, RHO-adRP. A transgenic mouse carrying a Pro347Ser mutant human RHO transgene[31] was bred onto a $Rho^{+/+}$ background ($RHO347^{+/-}Rho^{+/+}$) for this purpose. Mice were subretinally injected with AAVshQ1 and AAVshNT at postnatal day 10 and a viral spread of 10–20% was observed in these retinas (**Figure 4**). At 5 and 10 weeks postadministation, the outer nuclear layer (ONL) thickness in eyes treated with AAVshQ1 (**Figure 5b,e**) and AAVshNT (**Figure 5a,d**) was compared ($n = 3$–5). ONL measurements were taken in regions of retinas transduced by AAV, as defined by EGFP fluorescence, and significant differences were observed (**Figure 5g**). At 5 weeks postinjection, ONL thickness was 1.7-fold greater ($P < 0.001$) in eyes injected with AAVshQ1 (176.1 ± 55.5%) versus AAVshNT (100 ± 13.5%). Eyes injected with AAVshNT and uninjected eyes did not differ significantly (**Figure 5g**). At 10 weeks postinjection, ONL thickness was 2.1-fold greater ($P < 0.001$) in eyes injected with AAVshQ1 (91.3 ± 17.8%) versus AAVshNT (43.4 ± 11.7%). Note that all ONL thicknesses were compared to that of AAVshNT at 5 weeks. Again, eyes injected with AAVshNT and uninjected eyes were similar (**Figure 5g**). Employing antibodies either specific to human RHO or to both RHO and Rho indicated that subretinal administration of AAVshQ1 in Pro347Ser mice resulted specifically in suppression of mutant RHO while expression of Rho was

maintained (**Figure 6**). Notably, an associated preservation of retinal structure in eyes treated with AAVshQ1 versus AAVshNT was observed (**Figures 5b,e** and **6e–h**). These data demonstrate at the histological level that AAVshQ1 can suppress human RHO and beneficially modulate the retinopathy in Pro347Ser mice. In this regard, the level of human RHO expression in Pro347Ser mice is similar to the level of endogenous mouse Rho in wild-type mice (data not shown).

To determine whether AAVshQ1 leads to functional benefit in Pro347Ser mice, ERG was performed ($n = 15$) at 10 weeks postinjection on mice that had received AAVshQ1 and AAVshNT in fellow eyes at postnatal day 10 (**Figure 7a–f**). Significant improvements in rod-isolated, mixed rod and cone, and cone-isolated responses were observed in treated eyes. An overlay of ERGs from these mice is presented (**Figure 7a**). The average ERG values determined for eyes injected with AAVshQ1 versus AAVshNT were approximately twofold greater: rod-isolated responses(132.48 ± 80.56 µV and 75.67 ± 50.75 µV, respectively; $P < 0.01$), mixed rod and cone responses (277.47 ± 185.81 µV and 152.28 ± 106.51 µV, respectively; $P < 0.01$), and cone-isolated responses (79.67 ± 53.29 µV and 45.35 ± 27.27 µV, respectively, $P < 0.01$). While a significant improvement was observed in Pro347Ser mice, the ERGs were still substantially reduced from that in wild-type mouse eyes. The results indicate that suppression and replacement can improve function as evaluated by ERG in *RHO*-adRP mice.

In summary, a single subretinal injection of an AAV-delivered RNAi suppressor, AAVshQ1, has been shown to potently suppress human RHO mRNA and protein in NHR mice resulting in retinal degeneration and a significant reduction in ERG responses. More important, AAVshQ1-mediated RHO suppression in conjunction with expression of an endogenous replacement *RHO* gene in Pro347Ser mice slowed the retinal degeneration as demonstrated by significantly improved histology and ERG. These data provide evidence of RNAi-mediated therapeutic benefit in a transgenic mouse model that simulates human *RHO*-adRP and further validates the general approach of suppression and replacement for dominant conditions.

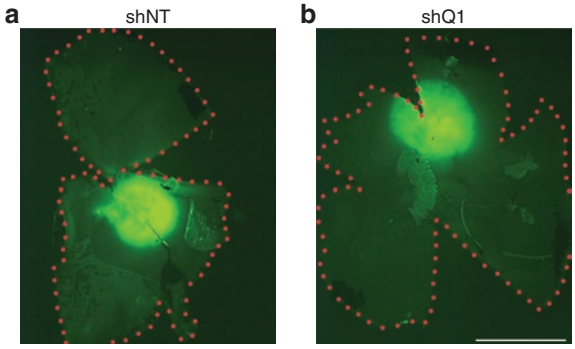

Figure 4 Viral spread in Pro347Ser mice. Fellow eyes from Pro347Ser ($RHO347^{+/-}Rho^{+/+}$) mice were injected with 1 µl of 2 × 10^{12} vp/ml AAVshQ1 and AAVshNT at postnatal day 10. Five weeks postinjection, eyes were fixed in 4% paraformaldehyde and retinal whole mounts prepared. Representative microscope images are depicted from eyes injected with AAVshNT (shNT; **a**) and AAVshQ1 (shQ1; **b**). Green label corresponds to EGFP fluorescence signal in the AAV-targeted region of the retina. Red dots border the extent of the retinas. Bar = 1 mm.

DISCUSSION

The majority of autosomal dominantly inherited diseases are mutationally heterogeneous (OMIM database). Development of gene-based therapies for these conditions, including *RHO*-adRP, represents a substantial challenge both technically and economically. Effective therapies targeted to correcting these disorders will typically require suppression of mutant alleles. Mutation-independent approaches such as suppression and replacement,[9–14] exploited in this study for *RHO*-adRP, are extremely valuable as a single therapeutic agent that may provide a remedy for many different mutant alleles of a disease gene. Although the strategy may also provide a rational solution for many dominant conditions, the application of the approach is complex, involving delivery of two-component nucleotide-based therapies. Given the inherent complexity of such therapies, RNAi-mediated suppression of RHO targeted to sites that differ in nucleotide sequence between mouse and human RHO, such that the endogenous mouse gene is resistant to suppression (thereby acting as a replacement gene), has been explored in this study. In this manner, the potency of

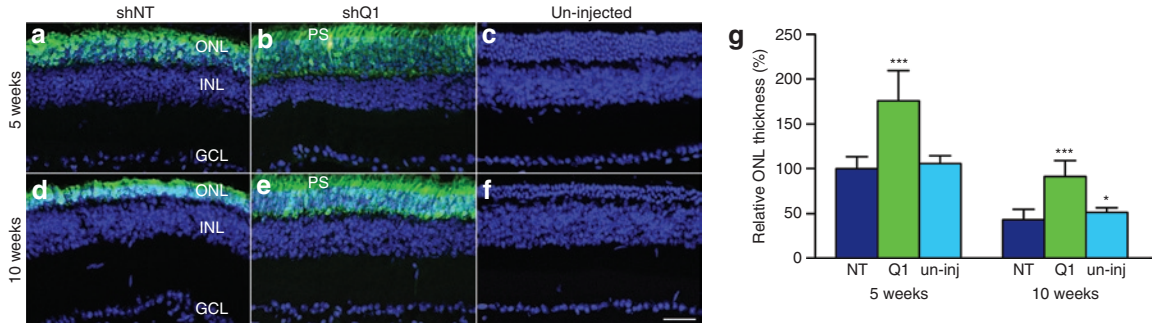

Figure 5 Retinal histology of Pro347Ser mice following subretinal administration of AAVshQ1 and AAVshNT. Fellow eyes from Pro347Ser ($RHO347^{+/-}Rho^{+/+}$) mice were injected with 1 µl of 2 × 10^{12} vp/ml AAVshQ1 and AAVshNT at postnatal day 10. Five and 10 weeks postinjection, eyes were fixed in 4% paraformaldehyde, cryosectioned (12 µm) and nuclei counterstained with DAPI. Representative microscope images are shown from eyes injected with (**a,d**) AAVshNT, (**b,e**) AAVshQ1, and (**c,f**) from uninjected eyes. Green label corresponds to EGFP fluorescence signal in the AAV-targeted region of the retina. Three measurements of ONL thickness were taken in each of two or three microscope images, 200 µm apart in the AAV-targeted area of each eye ($n = 3–5$). (**g**) Bars represent relative ONL thickness (normalized to 5-week AAVshNT-control eyes) at 5 or 10 weeks postinjection. PS, photoreceptor segments; INL, inner nuclear layer; GCL, ganglion cell layer. Bar = 25 µm. Error bars correspond to SD values; *$P < 0.05$; ***$P < 0.001$.

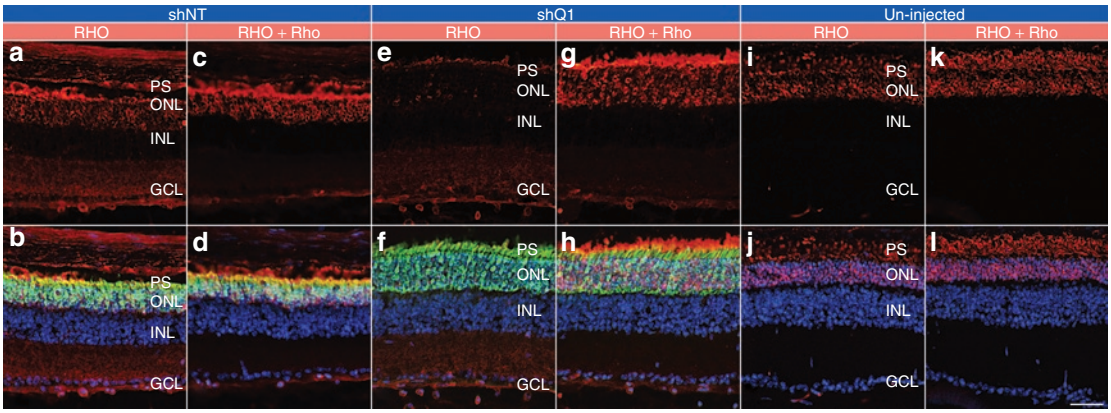

Figure 6 Selective suppression of RHO versus Rho expression in Pro347Ser retina. Fellow eyes of Pro347Ser ($RHO347^{+/-}Rho^{+/+}$) mice were injected with 1 µl of 2×10^{12} vp/ml AAVshQ1 and AAVshNT at postnatal day 10. Five weeks postinjection, eyes were fixed in 4% paraformaldehyde and cryosectioned (12 µm). Immunocytochemistry using human RHO-specific or RHO- and Rho-specific rhodopsin antibodies was carried out (using Cy3-conjugated secondary antibody) and nuclei counterstained with DAPI. Representative microscopic images are presented from eyes injected with (**a**, **b**, **c**, and **d**) AAVshNT, and (**e**, **f**, **g**, and **h**) AAVshQ1, or (**i**, **j**, **k**, and **l**) uninjected eyes. Green label corresponds to EGFP fluorescence signal in the AAV-targeted region of the retinas. The top row depicts rhodopsin signals (RHO and Rho) and the bottom row illustrates overlaid signals of rhodopsin, EGFP, and DAPI. Sections used for immunocytochemistries were from the same eye and were no >50 µm apart. PS, photoreceptor segments; ONL, outer nuclear layer; INL, inner nuclear layer; GCL, ganglion cell layer. Bar = 25 µm.

RNAi-based suppression to provide benefit can be evaluated independent of the delivery of a replacement gene. Indeed a similar experimental approach was adopted previously for the RNAi-mediated suppression of a mutant human ataxin-1 gene in conjunction with expression of the endogenous mouse *ataxin-1* gene for dominant Spinocerebellar Ataxia (SCA).[33] However, unlike RHO for adRP,[34] the absolute requirement of an ataxin-1 replacement gene for SCA has not been fully established.[33]

In this study, AAV vectors expressing RHO-targeting and nontargeting RNAi molecules were generated (AAVshQ1 and AAVshNT) and potent suppression of wild-type and mutant human RHO demonstrated. In NHR ($RHO^{+/-}Rho^{-/-}$) mice, a single subretinal administration of AAVshQ1 suppressed RHO (**Figures 2c** and **3**) and reduced ERG significantly (**Figure 3j**). Reduced cone responses were also observed in line with prior findings suggesting that loss of rod photoreceptors can result in reduced cone function.[35,36] Moreover, analysis of AAV-transduced cells isolated by FACS demonstated that shQ1 suppressed human RHO by 95% in NHR mice, whereas, in contrast, shQ1 did not suppress mouse Rho in wild-type mice (**Figure 2d**). This facilitated evaluation of suppression and replacement in the Pro347Ser transgenic mouse model for *RHO*-adRP. This mouse has an RHO mutation that has been observed in a number of *RHO*-adRP families.[37] Photoreceptor cell loss in the Pro347Ser mouse occurs over a 4-month period, potentially providing sufficient time for therapeutic intervention.[31] For the current study, the Pro347Ser mouse was bred onto a wild-type background; the resulting progency ($RHO347^{+/-}Rho^{+/+}$) express wild-type Rho that functions as a replacement gene for RHO due to mismatches over the target site for shQ1. Notably, a single subretinal administration of AAVshQ1 into Pro347Ser mice resulted in a significant retardation of the retinopathy as evaluated by histology and ERG (**Figures 5–7**). The slower retinopathy in the Pro347Ser animal model enabled evaluation of ERG, which contrasts with the previous study with Pro23His mice.[13]

It is worth emphasizing that RHO is expressed extremely highly in the retina.[38,39] An adult mouse retina is estimated to have

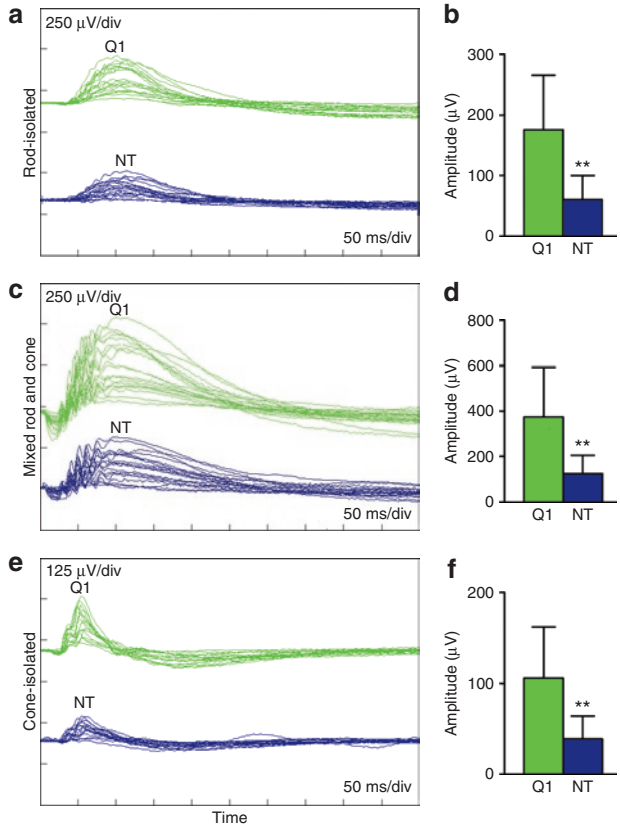

Figure 7 ERG of Pro347Ser mice following subretinal administration of AAVshQ1 and AAVshNT. Fellow eyes from Pro347Ser ($RHO347^{+/-}Rho^{+/+}$) mice were injected with 1 µl of 2×10^{12} vp/ml AAVshQ1 and AAVshNT at postnatal day 10 ($n = 15$). Ten weeks postinjection, mice were dark adapted overnight and (**a**,**b**) rod-isolated, (**c**,**d**) mixed rod and cone, and (**e**,**f**) cone-isolated ERG responses were recorded from both eyes. **a**, **c**, and **e**: ERGs, from eyes injected with AAVshQ1 (Q1: green) and AAVshNT (NT: blue). **b**, **d**, and **f**: mean ERG amplitudes. Error bars represent SD values; $^{**}P < 0.01$. Note that amplitudes on **a**, **c**, and **e**, and Y axes on **b**, **d**, and **e** are set to different scales.

6.4 million rod photoreceptor cells, each producing a steady-state level of 60 million RHO molecules (550–650 pmol; ref. 40), highlighting the need for potent suppressors, such as shQ1, delivered by efficient vectors, such as AAV2/5. Viral spread (*i.e.*, the transduced portion of the retina as assessed by EGFP expression) following subretinal injection of AAV in Pro347Ser mice was in the region of 10–20% (**Figure 4**), less than that observed in NHR and wild-type mice (30–40%). This may be a function of the retinal degeneration in Pro347Ser mice. Notably, even with a viral spread of 10–20% histological and ERG benefit has been observed in the current study. One may speculate that wider spread of the viral therapy in the target tissue may lead to greater therapeutic effects. A future challenge involves expression of therapeutically beneficial levels of RHO from AAV vectors carrying both suppression and replacement components.

The current study represents an *in vivo* demonstration that suppression and replacement may provide ERG benefit in an animal model of a dominant retinal disease. RNAi-mediated suppression of mutant RHO, in conjunction with the expression of an endogenous Rho refractory to suppression, provided therapeutic benefit to the Pro347Ser mouse. The results represent significant progress toward the development of two-component nucleotide-based therapies for *RHO*-adRP, which may be utilized to circumvent the mutational heterogeneity present in many other dominantly inherited conditions.

MATERIALS AND METHODS

AAV suppression constructs. The RHO-targeting short hairpin RNA shQ1 (target position nt 650–670; ref. 13) was cloned into pAAV-MCS (Stratagene, La Jolla, CA) with the EGFP reporter gene [pEGFP-1, BD Biosciences, Oxford, UK (Entrez Gene accession no. U57608)] to create pAAVshQ1 (**Figure 1**). shQ1 targets the RHO nucleotide sequence TCG TGT GGA ATC GAC TAC that differs from the mouse Rho sequence at four positions as underlined, TCA TGC GGG ATT GAC TAC, while encoding the same amino acids. Helper virus–free recombinant AAV2/5 viruses, containing either pAAVshQ1 or the nontargeting control construct pAAVshNT (NT: 5′ UUCUCCGAACGUGUCACGU 3′) were generated as previously described.[13] Genomic titers, that is, viral particles per milliliter (vp/ml), were determined by quantitative real-time PCR[41] and viral preparations diluted to 2×10^{12} vp/ml with PBS for use in this study.

Transgenic mouse models. Various mouse transgenic lines were utilized in the study including a mouse RHO knockout ($Rho^{-/-}$; ref. 34), NHR mice carrying a wild-type human RHO transgene (NHR[20]), and the Pro347Ser mouse model of adRP carrying a mutant human RHO transgene (RHO347; ref. 31). NHR mice were bred onto a $Rho^{-/-}$ background ($RHO^{+/-}Rho^{-/-}$; ref. 32), and Pro347Ser were bred onto a wild-type mouse RHO background ($RHO347^{+/-}Rho^{+/+}$) for this study. All animals were on a 129 S2/SvHsd (Harlan, Huntington, UK) background. Mice were maintained under specific pathogen-free housing conditions.

Subretinal AAV injection. Subretinal injections were carried out in strict compliance with the European Communities Regulations 2002 and 2005 (Cruelty to Animals Act) and ARVO statement for the use of animals in ophthalmic and vision research. Each mouse eye received a single subretinal injection. Mice were anesthetized by intraperitoneal injection of Medetomidine and Ketamine (10 and 750 μg/10 g body weight, respectively). Pupils were dilated with 1% cyclopentolate and 2.5% phenylephrine, and under local analgesia (amethocaine) a small puncture was made in the sclera. A 34-gauge blunt-ended microneedle attached to a 10-μl syringe (Hamilton Company Europe, Bonaduz, Switzerland) was inserted through the puncture and a single dose of AAV was administered to the subretinal space and a retinal detachment induced. Following surgery an anesthetic reversing agent (Atipamezole Hydrochloride, 100 μg/10 g body weight) was delivered by intraperitoneal injection. Body temperature was maintained using a homeothermic heating device.

Quantitative real-time RT-PCR and RNase protection assay. Following euthanasia, mouse neural retinas were harvested and trypsin dissociated, and retinal cells expressing EGFP were identified and sorted by FACS as described.[14] RNA was isolated using the RNeasy Mini Kit (Qiagen, Crawley, UK). Human RHO and mouse Rho mRNA expression levels were assessed by qRT-PCR using the following primer sequences from 5′–3′: RHO forward CTTTCCTGATCTGCTGGGTG, RHO reverse GGCAAAGAACGCTGGGATG, Rho forward TGTGGTCTTCACCTGG ATCAT, Rho reverse AATCCCGCATGAACATTGCAT.

Expression of shQ1 was determined by RNase protection assay as described[13] using the following RNA probe specific to shQ1, 5′ UAGUAGUCGAUUCCACACGAG 3′, labeled with P^{32}-γATP. Protected RNA was separated on 15% denaturing acrylamide gels and visualized by autoradiography.

Immunocytochemistry and microscopy. Retinas were dissected and flat mounted as described.[42] RHO immunocytochemistry and fluorescent microscopy were performed as described,[25] using Cy3-conjugated secondary antibody. For RHO-specific immunocytochemistry, 3A6 primary RHO antibody was used in 1:10 dilution.[43] ONL thickness was measured in three microscope images from each of two or three planes, 200 μm apart in the AAV-targeted area of each eye using Photoshop (Adobe Systems Europe, Glasgow, UK).

ERG. Animals were dark adapted overnight and all procedures were carried out under dim red light. For anesthesia, ketamine and xylazine (16 and 1.6 μg/10-g body weight, respectively) were injected intraperitoneally. Pupils were dilated with 1% cyclopentalate and 2.5% phenylephrine. Eyes were maintained in a proptosed position throughout the examination. Reference and ground electrodes were positioned subcutaneously, ~1 mm from the temporal canthus and anterior to the tail, respectively. The ERG responses were recorded simultaneously from both eyes by means of goldwire electrodes (Roland Consulting, Brandenburg-Wiesbaden, Germany), which were positioned to touch the central cornea of each eye. Corneal hydration was maintained throughout the examination by the application of a small drop of vidisic (Dr Mann Pharma, Berlin, Germany) to the cornea. Standardized flashes of light were presented to the mouse in a Ganzfeld bowl. Responses were analyzed using a RetiScan RetiPort electrophysiology unit (Roland Consulting). The protocol used was based on the methods approved by the International Clinical Standards Committee for human ERG. Rod-isolated responses were recorded using a dim white flash (−25 dB maximal intensity where maximal flash intensity was three candelas/m^2/s) presented in the dark-adapted state. Maximal combined rod–cone response to the maximal-intensity flash was then recorded. Following a 10-minute light adaptation to a background illumination of 30 candelas/m^2, cone-isolated responses were recorded to the maximal-intensity flash presented initially as a single flash and subsequently as 10 Hz flickers. Following the standard convention, a-waves were measured from the baseline to the trough and b-waves from the baseline (in the case of rod-isolated responses) or from the a-wave trough.

Statistical analysis. Means, SD values, and Student's *t*-tests were calculated. Differences with $P < 0.05$ were considered statistically significant.

WEB RESOURCES

Accession numbers and URLs for data presented herein are a follows:

Entrez Gene, http://www.ncbi.nlm.nih.gov/entrez/ [for EGFP (accession no. U57608)]

GenBank, http://www.ncbi.nlm.nih.gov/Genbank/ [for RHO (accession no. NM_000539.2) and for Rho (accession no. M55171.1)]

Online Mendelian Inheritance in Man (OMIM), http://www.ncbi.nlm.nih.gov.Omim, for RP

Retinal Information Network database, http://www.sph.uth.tmc.edu/Retnet/

ACKNOWLEDGMENTS

We thank Prof. Thaddeus Dryja (Harvard Medical School, Massachusetts Eye and Ear Infirmary, Boston) for providing the NHR mouse; Dr Fernandez (Flow Cytometry Core Facility in University College, Dublin) for assisting with FACS analysis; Prof. R.S. Molday (University of British Colombia, Vancouver BC, CA) for the two rhodopsin primary antibodies; and the staff of the Bioresources Unit, Trinity College, Dublin. The research was supported by grant awards from Science Foundation Ireland, Fighting Blindness Ireland, Enterprise Ireland, the 6th Framework Programs of the European Union (RETNET MRT-CT-2003-504003, EviGenoRet LSHG-CT-2005-512036).

REFERENCES

1. Bainbridge, JW, Smith, AJ, Barker, SS, Robbie, S, Henderson, R, Balaggan, K *et al.* (2008). Effect of gene therapy on visual function in Leber's congenital amaurosis. *N Engl J Med* **358**: 2231–2239.
2. Maguire, AM, Simonelli, F, Pierce, EA, Pugh, EN Jr., Mingozzi, F, Bennicelli, J *et al.* (2008). Safety and efficacy of gene transfer for Leber's congenital amaurosis. *N Engl J Med* **358**: 2240–2248.
3. Hauswirth, W, Aleman, TS, Kaushal, S, Cideciyan, AV, Schwartz, SB, Wang, L *et al.* (2008). Phase I trial of Leber congenital amaurosis due to RPE65 mutations by ocular subretinal injection of adeno-associated virus gene vector: short-term results. *Hum Gene Ther* **19**: 979–990.
4. Perche, O, Doly, M and Ranchon-Cole, I (2007). Caspase-dependent apoptosis in light-induced retinal degeneration. *Invest Ophthalmol Vis Sci* **48**: 2753–2759.
5. Buch, PK, MacLaren, RE, Durán, Y, Balaggan, KS, MacNeil, A, Schlichtenbrede, FC *et al.* (2006). In contrast to AAV-mediated Cntf expression, AAV-mediated Gdnf expression enhances gene replacement therapy in rodent models of retinal degeneration. *Mol Ther* **14**: 700–709.
6. Tuohy, G, Millington-Ward, S, Kenna, PF, Humphries, P and Farrar, GJ (2002). Sensitivity of photoreceptor-derived cell line (661W) to baculoviral p35, Z-VAD.FMK, and Fas-associated death domain. *Invest Ophthalmol Vis Sci* **43**: 3583–3589.
7. Komeima, K, Rogers, BS, Lu, L and Campochiaro, PA (2006). Antioxidants reduce cone cell death in a model of retinitis pigmentosa. *Proc Natl Acad Sci USA* **103**: 11300–11305.
8. Phillips, MJ, Walker, TA, Choi, HY, Faulkner, AE, Kim, MK, Sidney, SS *et al.* (2008). Tauroursodeoxycholic acid preservation of photoreceptor structure and function in the rd10 mouse through postnatal day 30. *Invest Ophthalmol Vis Sci* **49**: 2148–2155.
9. Millington-Ward, S, O'Neill, B, Tuohy, G, Al-Jandal, N, Kiang, AS, Kenna, PF *et al.* (1997). Strategems *in vitro* for gene therapies directed to dominant mutations. *Hum Mol Genet* **6**: 1415–1426.
10. Hauswirth, WW and Lewin, AS (2000). Ribozyme uses in retinal gene therapy. *Prog Retin Eye Res* **9**: 689–710.
11. Kim, DH and Rossi, JJ (2003). Coupling of RNAi-mediated target downregulation with gene replacement. *Antisense Nucleic Acid Drug Dev* **13**: 151–155.
12. Cashman, SM, Binkley, EA and Kumar-Singh, R (2005). Towards mutation-independent silencing of genes involved in retinal degeneration by RNA interference. *Gene Ther* **12**: 1223–1228.
13. O'Reilly, M, Palfi, A, Chadderton, N, Millington-Ward, S, Ader, M, Cronin, T *et al.* (2007). RNA interference-mediated suppression and replacement of human rhodopsin *in vivo*. *Am J Hum Genet* **81**: 127–135.
14. Palfi, A, Ader, M, Kiang, AS, Millington-Ward, S, Clark, G, O'Reilly, M *et al.* (2006). RNAi-based suppression and replacement of rds-peripherin in retinal organotypic culture. *Hum Mutat* **27**: 260–268.
15. Farrar, GJ, Kenna, PF and Humphries, P (2002). On the genetics of retinitis pigmentosa and on mutation-independent approaches to therapeutic intervention. *EMBO J* **21**: 857–864.
16. McWilliam, P, Farrar, GJ, Kenna, P, Bradley, DG, Humphries, MM, Sharp, EM *et al.* (1989). Autosomal dominant retinitis pigmentosa (ADRP): localization of an ADRP gene to the long arm of chromosome 3. *Genomics* **5**: 619–622.
17. Farrar, GJ, McWilliam, P, Bradley, DG, Kenna, P, Lawler, M, Sharp, EM *et al.* (1990). Autosomal dominant retinitis pigmentosa: linkage to rhodopsin and evidence for genetic heterogeneity. *Genomics* **8**: 35–40.
18. Dryja, TP, McGee, TL, Reichel, E, Hahn, LB, Cowley, GS, Yandell, DW *et al.* (1990). A point mutation of the rhodopsin gene in one form of retinitis pigmentosa. *Nature* **343**: 364–366.
19. Mendes, HF and Cheetham, ME (2008). Pharmacological manipulation of gain-of-function and dominant-negative mechanisms in rhodopsin retinitis pigmentosa. *Hum Mol Genet* **17**: 3043–3054.
20. Olsson, JE, Gordon, JW, Pawlyk, BS, Roof, D, Hayes, A, Molday, RS *et al.* (1992). Transgenic mice with a rhodopsin mutation (Pro23His): a mouse model of autosomal dominant retinitis pigmentosa. *Neuron* **9**: 815–830.
21. Lewin, AS, Drenser, KA, Hauswirth, WW, Nishikawa, S, Yasumura, D, Flannery, JG *et al.* (1998). Ribozyme rescue of photoreceptor cells in a transgenic rat model of autosomal dominant retinitis pigmentosa. *Nat Med* **8**: 967–971.
22. LaVail, MM, Yasumura, D, Matthes, MT, Drenser, KA, Flannery, JG, Lewin, AS *et al.* (2000). Ribozyme rescue of photoreceptor cells in P23H transgenic rats: long-term survival and late-stage therapy. *Proc Natl Acad Sci USA* **97**: 11488–11493.
23. Tessitore, A, Parisi, F, Denti, MA, Allocca, M, Di Vicino, U, Domenici, L *et al.* (2006). Preferential silencing of a common dominant rhodopsin mutation does not inhibit retinal degeneration in a transgenic model. *Mol Ther* **14**: 692–699.
24. O'Neill, B, Millington-Ward, S, O'Reilly, M, Tuohy, G, Kiang, AS, Kenna, PF *et al.* (2000). Ribozyme based therapeutic approaches for autosomal dominant retinitis pigmentosa. *Invest Opthalmol Vis Sci* **41**: 2863–2869.
25. Gorbatyuk, M, Justilien, V, Liu, J, Hauswirth, WW and Lewin, AS (2007). Preservation of photoreceptor morphology and function in P23H rats using an allele independent ribozyme. *Exp Eye Res* **84**: 44–52.
26. Kiang, AS, Palfi, A, Ader, M, Kenna, PF, Millington-Ward, S, Clark, G *et al.* (2005). Toward a gene therapy for dominant disease: validation of an RNA interference-based mutation-independent approach. *Mol Ther* **12**: 555–561.
27. O'Reilly, M, Millington-Ward, S, Palfi, A, Chadderton, N, Cronin, T, McNally, N *et al.* (2008). A transgenic mouse model for gene therapy of rhodopsin-linked Retinitis Pigmentosa. *Vision Res* **48**: 386–391.
28. Auricchio, A, Kobinger, G, Anand, V, Hildinger, M, O'Connor, E, Maguire, AM *et al.* (2001). Exchange of surface proteins impacts on viral vector cellular specificity and transduction characteristics: the retina as a model. *Hum Mol Genet* **10**: 3075–3081.
29. Lotery, AJ, Yang, GS, Mullins, RF, Russell, SR, Schmidt, M, Stone, EM *et al.* (2003). Adeno-associated virus type 5: transduction efficiency and cell-type specificity in the primate retina. *Hum Gene Ther* **14**: 1663–1671.
30. Allocca, M, Doria, M, Petrillo, M, Colella, P, Garcia-Hoyos, M, Gibbs, D *et al.* (2008). Serotype-dependent packaging of large genes in adeno-associated viral vectors results in effective gene delivery in mice. *J Clin Invest* **118**: 1955–1964.
31. Li, T, Snyder, WK, Olsson, JE and Dryja, TP (1996). Transgenic mice carrying the dominant rhodopsin mutation P347S: evidence for defective vectorial transport of rhodopsin to the outer segments. *Proc Natl Acad Sci USA* **93**: 14176–14181.
32. McNally, N, Kenna, P, Humphries, MM, Hobson, AH, Khan, NW, Bush, RA *et al.* (1999). Structural and functional rescue of murine rod photoreceptors by human rhodopsin transgene. *Hum Mol Genet* **8**: 1309–1312.
33. Xia, H, Mao, Q, Eliason, SL, Harper, SQ, Martins, IH, Orr, HT *et al.* (2004). RNAi suppresses polyglutamine-induced neurodegeneration in a model of spinocerebellar ataxia. *Nat Med* **10**: 816–820.
34. Humphries, MM, Rancourt, D, Farrar, GJ, Kenna, P, Hazel, M, Bush, RA *et al.* (1997). Retinopathy induced in mice by targeted disruption of the rhodopsin gene. *Nat Genet* **15**: 216–219.
35. Humphries, MM, Kiang, S, McNally, N, Donovan, MA, Sieving, PA, Bush, RA *et al.* (2001). Comparative structural and functional analysis of photoreceptor neurons of $Rho^{-/-}$ mice reveal increased survival of C57BL/6J in comparison to 129Sv genetic background. *Vis Neurosci* **18**: 437–443.
36. Léveillard, T, Mohand-Saïd, S, Lorentz, O, Hicks, D, Fintz, AC, Clérin, E *et al.* (2004). Identification and characterization of rod-derived cone viability factor. *Nat Genet* **36**: 755–759.
37. Daiger, SP, Sullivan, LS and Rodriguez, JA (1995). Correlation of phenotype with genotype in inherited retinal degeneration. *Behavioral Brain Sci* **18**: 491–506.
38. Lyubarsky, AL, Daniele, LL and Pugh, EN Jr. (2004). From candelas to photoisomerizations in the mouse eye by rhodopsin bleaching *in situ* and the light-rearing dependence of the major components of the mouse ERG. *Vision Res* **44**: 3235–3251.
39. Unger, VM, Hargrave, PA, Baldwin, JM and Schertler, GF (1997). Arrangement of rhodopsin transmembrane α-helices. *Nature* **389**: 203–206.
40. Wensel, TG, Gross, AK, Chan, F, Sykoudis, K and Wilson, JH (2005). Rhodopsin-EGFP knock-ins for imaging quantal gene alterations. *Vision Res* **45**: 3445–3453.
41. Rohr, UP, Wulf, MA, Stahn, S, Steidl, U, Haas, R and Kronenwett, R (2002). Fast and reliable titration of recombinant adeno-associated virus type-2 using quantitative real-time PCR. *J Virol Methods* **106**: 81–88.
42. D'Amato, R, Wesolowski, E and Smith, LE (1993). Microscopic visualization of the retina by angiography with high-molecular-weight fluorescein-labeled dextrans in the mouse. *Microvasc Res* **46**: 135–142.
43. MacKenzie, D, Arendt, A, Haregrave, P, McDowell, JH and Molday, RS (1984). Localization of binding sites for carboxyl terminal specific anti-fhodopsin monoclonal antibodies using synthetic peptides. *Biochemistry* **23**: 6544–6549.